Inorganic Chemistry

Forum Article

Cite This: Inorg. Chem. XXXX, XXX, XXX−XXX

pubs.acs.org/IC

Four-Component Catalytic Machinery: Reversible Three-State Control of Organocatalysis by Walking Back and Forth on a Track

Nikita Mittal, Merve S. Özer, and Michael Schmittel*

Center of Micro and Nanochemistry and Engineering, Organische Chemie I, Universität Siegen, Adolf-Reichwein-Strasse 2, D-57068 Siegen, Germany

Supporting Information

ABSTRACT: A three-component supramolecular walker system is presented where a two-footed ligand (biped) walks back and forth on a tetrahedral 3D track upon the addition and removal of copper(I) ions, respectively. The addition of *N*-methylpyrrolidine as a catalyst to the walker system generates a four-component catalytic machinery, which acts as a three-state switchable catalytic ensemble in the presence of substrates for a conjugate addition. The copper(I)-ion-initiated walking process of the biped ligand on the track regulates the catalytic activity in three steps: ON versus ^{int}ON (intermediate ON) versus OFF. To establish the operation of the four-component catalytic machinery in a mixture of all constituents, forward and backward cycles were performed in situ illustrating that both the walking process and catalytic action are fully reversible and reproducible.

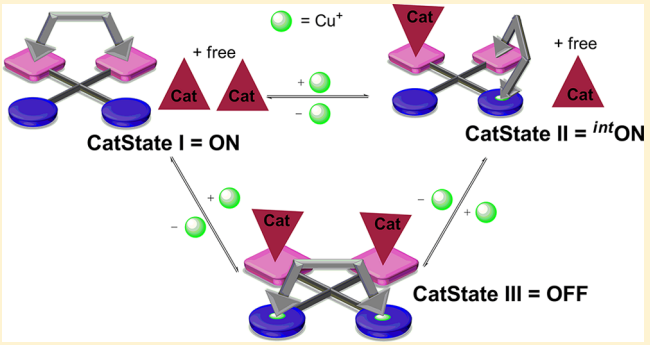

INTRODUCTION

Nature's design of protein-based molecular walkers (dynein, kinesin, and myosin) is amazing.[1] These startling systems walk step by step on microtubule or actin filament tracks, with each step driven by adenosine triphosphate hydrolysis, thereby executing essential tasks such as cargo transport, muscle contraction, cell division, etc.[2−6] They utilize weak noncovalent interactions like hydrogen bonding, electrostatic interactions, etc., to attach each foot to the track. Inspired by these biomolecular machines, several synthetic molecular walker systems, for instance based on dynamic covalent bond formation and cleavage, have been designed to mimic the walking process while keeping the directionality and processivity of the system intact.[7−14] Alternatively, labile transition-metal coordination motifs[15] have been utilized by Leigh's group[16] in preparing a two-footed ligand (biped) consisting of a platinum(II) complex as the kinetically inert foot and a palladium(II) complex as the labile foot, with the latter being able to step back and forth on the track via reversible protonation. At present, such walker systems using dynamic metal−ligand coordination remain scarce, although detachment of the foot from the track can be more easily accomplished than that with covalent systems.

Among the known artificial walker systems,[7] very few have been successfully coupled with additional functions, like fluorescence quenching,[17] although the processivity could be used for sequence-specific functionalization.[18] On the basis of our experience with allosteric artificial switches that are able to regulate catalytic processes such as click cycloaddition, cyclopropanation, Knoevenagel reactions, etc.,[19−21] we present a three-component walker system that is based on self-sorted metal−ligand interactions[22,23] and capable of controlling a conjugate addition depending on its position on the track when a proper catalyst is added. As demonstrated below, the walker **2** is able to walk reversibly on the four-station track **1** upon the addition and removal of copper(I) ions requiring a sophisticated stoichiometry-dependent self-sorting (Chart 1).[24,25]

In detail, the three-component system is composed of track **1** with its four binding sites [two sterically hindered phenanthrolines ($phenAr_2$) and two zinc(II) porphyrin (ZnPor) sites], the biped ligand **2**, and copper(I) ions (Scheme 1). In the absence of copper(I) ions, the biped ligand **2** with its two 2-methylpyridine binding terminals will coordinate to both ZnPor sites of track **1**. Upon the addition of copper(I) ions, the biped ligand **2** is expected to depart in two steps from the two ZnPor stations of **1** and thus walk toward the copper(I)-filled phenanthroline stations. The removal of copper will reverse the process. The addition of a catalyst to the three-component walker generates the four-component catalytic machinery. When this machinery is commanded to undergo stepwise walking in a solution containing the substrates for the catalytic process, then three-state catalysis emerges with ON versus ^{int}ON (intermediate ON) versus OFF activity.

Special Issue: Self-Assembled Cages and Macrocycles

Received: October 24, 2017

DOI: 10.1021/acs.inorgchem.7b02703
Inorg. Chem. XXXX, XXX, XXX−XXX

Chart 1. Track 1 and Biped 2

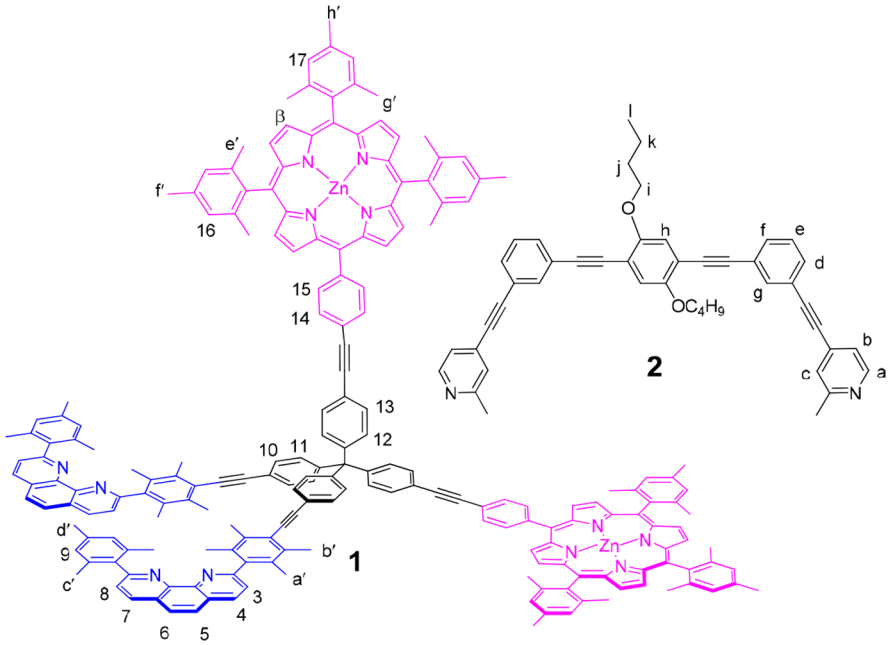

Scheme 1. Reversible Stepwise Walking of Biped 2 on the Tetrahedral Track 1, Forming Different States upon the Addition and Removal of Cu^+ Metal Ions

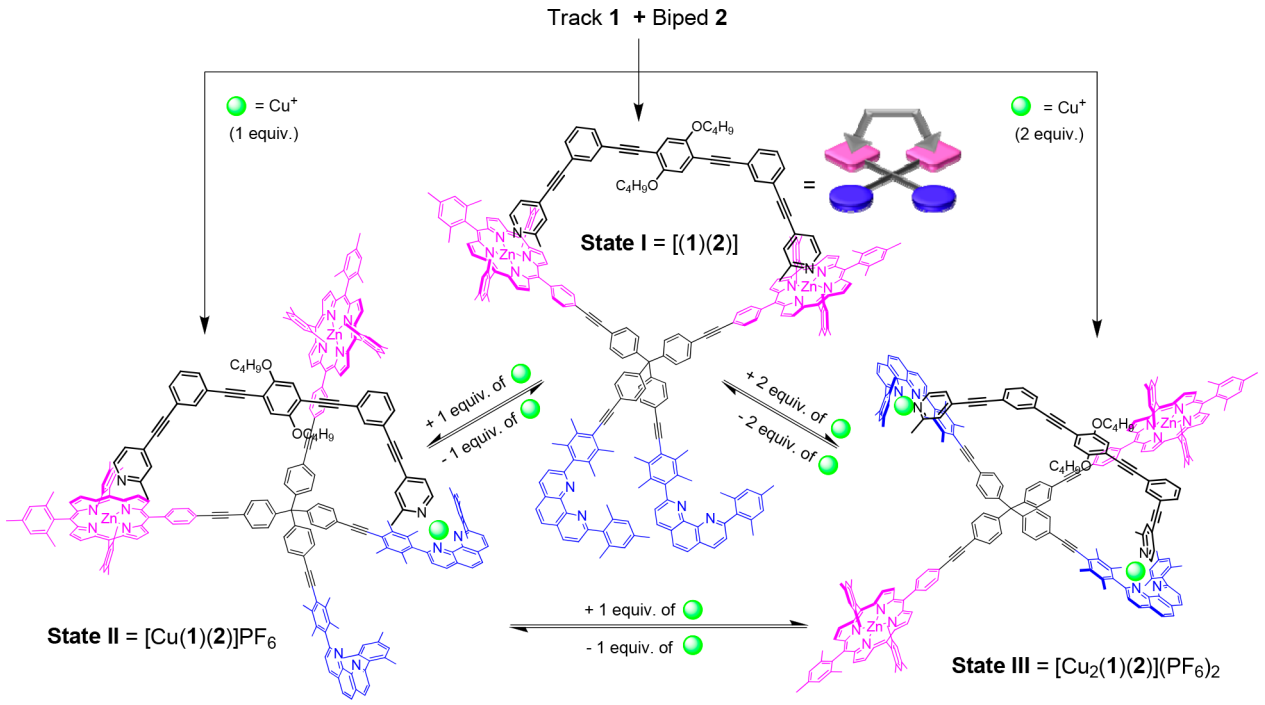

RESULTS AND DISCUSSION

Design. The structural design of the present four-component catalytic machinery was inspired by recent insights gained from our nanorotor[26,27] and nanoswitch[19−21] work. For instance, in a recently elaborated nanoswitch system,[20] the pyridylpyrimidine switching arm binds intramolecularly either to a ZnPor [in the absence of copper(I) ions] or to a $phenAr_2$ unit [in the presence of copper(I) ions], which allows control of catalyst release from the ZnPor unit into solution. The release is based on the fact that ZnPor systems can only accommodate one additional ligand;[28−30] thus, in the nanoswitch, ZnPor is intermolecularly bound either to the catalyst (usually a secondary amine) or to an intramolecular pyridine arm.

The conception of the four-component catalytic machinery is required to reconcile the operation of a three-component walker with the catalyst release as developed in our nanoswitch work. Track **1** was thus designed to provide a tetrahedral arrangement of two identical ZnPor and two sterically shielded phenanthroline ($phenAr_2$) stations. In state I, two $N_{Mepy} \rightarrow$ ZnPor interactions ensure the formation of complex [(**1**)(**2**)]. The $phenAr_2$ ligands are required for the uptake of copper(I)

DOI: 10.1021/acs.inorgchem.7b02703
Inorg. Chem. XXXX, XXX, XXX−XXX

Chart 2. Ligands 3−7 and Complexes C1−C3

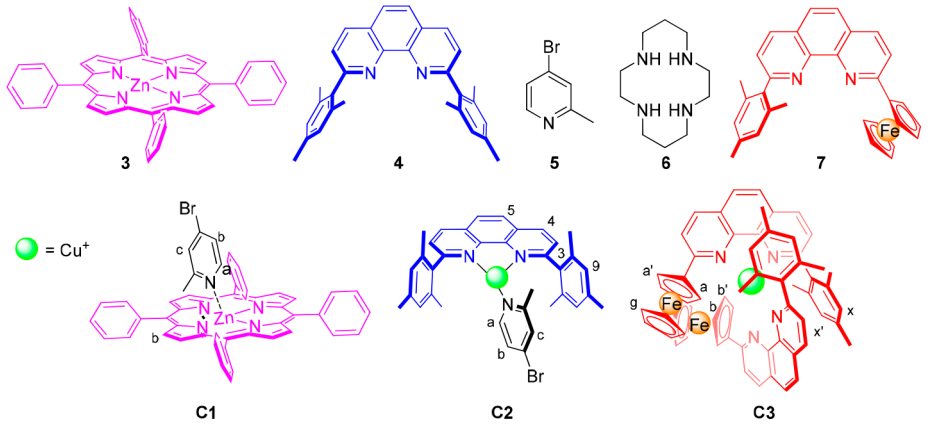

ions. Their steric shielding is a prerequisite to guarantee clean $N_{Mepy} \rightarrow [Cu(phenAr_2)]^+$ complexation[31] (HETPYP = heteroleptic pyridine and phenanthroline complexation) upon the addition of copper(I) ions to **1**.

The walking process needs a distinct thermodynamic driving force for the biped to move from ZnPor to the $[Cu(phenAr_2)]^+$ site. After various model studies with different pyridine derivatives, we decided on 2-methylpyridine as the terminal for the biped ligand **2** because it binds significantly with both binding units, i.e., with $[Cu(phenAr_2)]^+$ ($\log K = 3.43 \pm 0.01$; Figure S42) and ZnPor ($\log K = 2.3$[32]), which are available on track **1**. The required clean self-sorting upon going from [(**1**)(**2**)] to $[Cu(\mathbf{1})(\mathbf{2})]^+$ was tested ahead of finalizing the structural design of the track and biped. For instance, complex **C1** formed from zinc porphyrin **3** and 4-bromo-2-methylpyridine (**5**) mixed in a 1:1 ratio (Chart 2). In the ^{1}H NMR spectrum, the signals of protons a- and b-H are shifted upfield from 8.38 and 7.28 ppm in **5** to 6.44 and 6.81 ppm in **C1**, respectively, because of the protons' immersion in the porphyrin's ring current (Figure S9). In the ^{1}H NMR spectrum of complex **C2**, prepared by mixing ligands **4** and **5** and $[Cu(CH_3CN)_4]PF_6$ in a 1:1:1 ratio in CD_2Cl_2, characteristic upfield shifts of proton 9-H of ligand **4** from 6.93 to 6.74 ppm and proton a-H of ligand **5** from 8.38 to 7.61 ppm are seen (Figure S11). Complex **C2** was further characterized by electrospray ionization mass spectrometry (ESI-MS), which shows a single peak at m/z 652.0 for $[Cu(\mathbf{4})(\mathbf{5})]^+$ (Figure S39).

Another control ensured that the intramolecular 2-methylpyridine unit of **2** is a better binder to the ZnPor subunit of **1** than the intermolecularly present catalyst, *N*-methylpyrrolidine. This finding suggests that in the presence of complex [(**1**)(**2**)] the catalyst is available in solution.

Synthesis and Characterization of a Three-Component Walker. We synthesized the tetrahedral track **1** consisting two $phenAr_2$ and two ZnPor units as stations (Chart 1) via a series of Sonogashira coupling steps; details are mentioned in the Supporting Information (SI). Equally, several Sonogashira coupling reactions were used to synthesize the biped ligand **2** (Chart 1) with 2-methylpyridine units as terminals. Both compounds were fully characterized by spectroscopic techniques, i.e., ^{1}H NMR, ^{13}C NMR, DOSY NMR, ESI-MS, and elemental analysis (see the SI). Before studying the in situ three-state walking of the biped ligand **2** from the ZnPor to $phenAr_2$ stations of **1**, we decided to individually characterize each walking state. State I was prepared by mixing track **1** and biped ligand **2** in a 1:1 ratio in CD_2Cl_2. As expected, the formation of complex $[(\mathbf{1})(\mathbf{2})]$ is confirmed by strong upfield shifts of protons a-, b-, and c-H of the biped ligand **2** from 8.47, 7.21, and 7.28 ppm to 5.98, 6.52, and 6.61 ppm, respectively, due to immersion of those protons in the π ring cloud of the ZnPor stations of track **1** (Figure S13). Formation was additionally established by UV−vis data (Figure S41) because the Q band exhibits a 10 nm shift from 550 nm (track **1**) to 560 nm (state I), similar to that in other $N_{py} \rightarrow$ ZnPor interactions.[19] Complex $[(\mathbf{1})(\mathbf{2})]$ is further characterized by ^{1}H DOSY NMR, showing a single species with diffusion coefficient $D = 3.5 \times 10^{-10}$ m^2 s^{-1} ($r \sim 15.1$ Å) and confirming clean formation (Figure S32).

To prepare state III, i.e., $[Cu_2(\mathbf{1})(\mathbf{2})]^{2+}$, track **1**, biped ligand **2**, and $[Cu(CH_3CN)_4]PF_6$ were mixed in a 1:1:2 ratio. As anticipated, ^{1}H NMR analysis shows the characteristic upfield shifts of $phenAr_2$ protons 9-H from 6.96 ppm (in track **1**) to 6.71 ppm and of 2-methylpyridine protons a-H from 8.47 ppm (in biped **2**) to 7.52 ppm, suggesting the formation of a $[Cu(phenAr_2)(2\text{-methylpyridine})]^+$ complex unit (Figure S17). Indeed, a comparison of the ^{1}H NMR data of $[Cu_2(\mathbf{1})(\mathbf{2})]^{2+}$ with that of complex **C2** confirms the binding of both 2-methylpyridine terminals of biped ligand **2** to the $Cu^I phenAr_2$ stations of **1** (Figure S18). In agreement with this assignment, the Q band of state III is shifted back to 550 nm (Figure S41), i.e., to the same position as that in track **1**. ESI-MS of the mixture shows a single peak at m/z 1829.1 for $[Cu_2(\mathbf{1})(\mathbf{2})]^{2+}$, suggesting the quantitative formation of state III (Figure S40). A single set of signals in the ^{1}H DOSY NMR at $D = 3.36 \times 10^{-10}$ m^2 s^{-1} ($r \sim 15.7$ Å) further confirms our claim (Figure S34).

After the successful formation of states I and III of the walking system, we interrogated the crucial state II, i.e., $[Cu(\mathbf{1})(\mathbf{2})]^+$, because it requires a stoichiometry-dependent self-sorting. Thus, a CD_2Cl_2 solution of track **1**, biped ligand **2**, and $[Cu(CH_3CN)_4]PF_6$ in a 1:1:1 ratio was subjected to ^{1}H NMR measurement without any purification. Two types of mesityl protons 9-H emerge, one for the complexed $phenAr_2$ unit at 6.72 and 6.75 ppm and the other for the uncomplexed $phenAr_2$ unit at 6.96 and 6.95 ppm (Figure S15). The two sets of signals are actually strong support for the identity of state II. Two racemic diastereomers are expected because the central carbon and the $N_{Mepy} \rightarrow [Cu(phenAr_2)]^+$ linkage are stereogenic. Since all peaks of track **1** (complexed as well as uncomplexed sites) show up in two sets at a 1:1 ratio, the formation of two diastereomers is warranted in a 1:1 ratio. Reciprocally, a mixture of states I and III rather than state II is

DOI: 10.1021/acs.inorgchem.7b02703
Inorg. Chem. XXXX, XXX, XXX−XXX

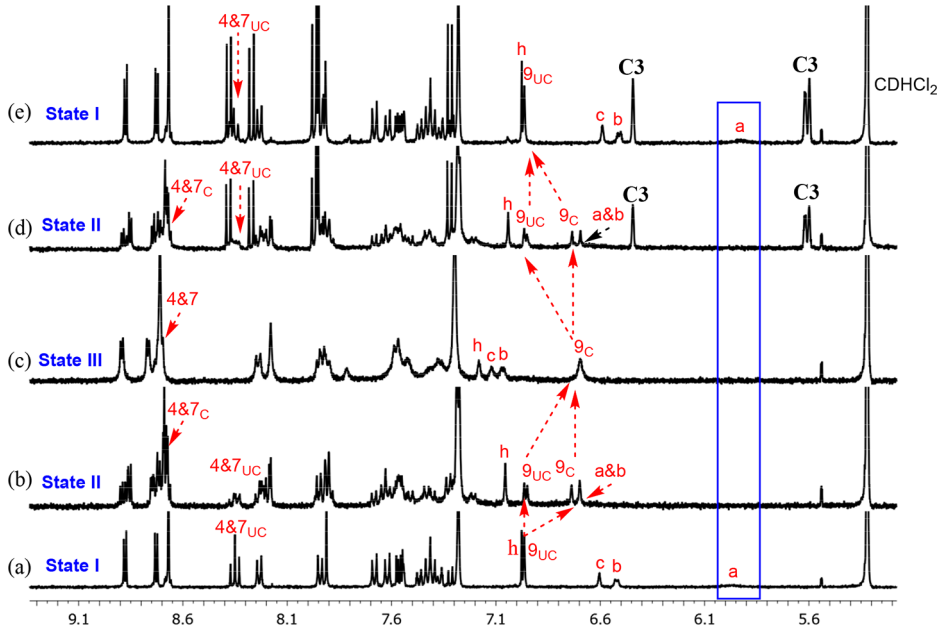

Figure 1. ^{1}H NMR (400 MHz, 298 K, CD_2Cl_2) showing in situ reversible stepwise walking of biped **2** on track **1** upon the sequential addition and removal of Cu^+ ions, thereby switching between different states of the system; (a) state I ([(**1**)(**2**)]) obtained after mixing track **1** and biped **2** in a 1:1 ratio; (b) the addition of 1 equiv of $[Cu(CH_3CN)_4]PF_6$ to state I depicted in spectrum a generates state II, i.e., $[Cu(\mathbf{1})(\mathbf{2})]PF_6$; (c) the addition of 1 equiv more of $[Cu(CH_3CN)_4]PF_6$ to state II depicted in spectrum b generates state III, i.e., $[Cu_2(\mathbf{1})(\mathbf{2})](PF_6)_2$; (d) the addition of 2 equiv of ligand **7** to state III displayed in spectrum c to remove 1 equiv of Cu^+ regenerates state II and complex **C3**; (e) the addition of 2 equiv more of ligand **7** to remove the remaining Cu^+ regenerates state I along with complex **C3**. The subscripts UC and C denote uncomplexed and complexed sites.

ruled out by the presence of two ^{1}H NMR sets. In the case of a mixture, the complexed and uncomplexed sites should display a single set each. The identity of $[Cu(\mathbf{1})(\mathbf{2})]^+$ is additionally substantiated by UV−vis data (Figure S41) as the Q band shifted from 550 nm (track **1**) to 554 nm (state II).[33] Furthermore, a single peak in the DOSY NMR with a diffusion coefficient $D = 3.44 \times 10^{-10}$ m^2 s^{-1} ($r \sim 15.3$ Å) suggests clean formation of state II (Figure S33).

The clean formation of all states suggested to study in situ the reversible walking of the walker system (Scheme 1) depending on the copper(I) ion stoichiometry. Initially, track **1** and biped ligand **2** were mixed in a 1:1 ratio in CD_2Cl_2 to form state I with both feet at the ZnPor stations of track **1** (Figure 1a). Now, upon the addition of 1 equiv of $[Cu(CH_3CN)_4]PF_6$ to state I, the ^{1}H NMR demonstrates the formation of state II; thus, one foot of ligand **2** has walked to one of the free $phenAr_2$ stations of track **1** (Figure 1b). After the addition of a further 1 equiv of $[Cu(CH_3CN)_4]PF_6$ into the latter solution, the ^{1}H NMR (Figure 1c) confirms that ligand **2** is now attached to both copper(I)-filled $phenAr_2$ stations of track **1**, representing state III. Thus, the designed two-step walking of ligand **2** from ZnPor stations to $phenAr_2$ stations of **1** has taken place.

After the two forward walking steps by the sequential addition of copper(I) ions were realized, the reverse walking was studied by removing them. We used the electron-rich 2-ferrocenyl-9-mesityl-1,10-phenanthroline (**7**) to remove copper(I) ions because it forms the highly stable homoleptic complex $[Cu(\mathbf{7})_2]^+$ (**C3**; log K = 11.0;[34] Chart 2). The addition of 2 equiv of ligand **7** (Chart 2) to state III leads to the formation of state II (Figure 1d) within seconds. Thus, the high dynamics about the $N_{Mepy} \rightarrow [Cu(phenAr_2)]^+$ binding, as established already earlier in other systems,[24] allows the fast trapping of 1 equiv of copper(I) ions by **7** and thus the rapid movement of one foot of ligand **2** from $phenAr_2$ to the ZnPor station on track **1**. The addition of 2 equiv more of ligand **7** causes walking of ligand **2** back to both ZnPor sites, regenerating state I (Figure 1e). Thus, as anticipated by our design, the system was reversed in a stepwise process (Figure 1d,e) without any loss.

Four-Component Catalytic Machinery. After establishing the full reversibility of the walker, we decided to transform the walker into four-component catalytic machinery. As delineated above in the design chapter,[15] we envisioned that the ZnPor units present in the walking system may be programmed to capture or release catalytically active secondary amines, such as piperidine[20] or *N*-methylpyrrolidine,[35] by the addition or removal of copper(I) ions. In the presence of the substrates for an organocatalytic reaction, stepwise regulation of catalysis (ON, ^{int}ON, and OFF) should be possible by addressing the various states I−III.

For instance, as long as biped ligand **2** is bound to both ZnPor stations in [(**1**)(**2**)], all of the added catalyst should be available in solution, resulting in 100% activity (ON state). Upon the addition of 1 equiv of copper(I) ions to this solution, the formation of $[Cu(\mathbf{1})(\mathbf{2})]^+$ will take place, where one liberated ZnPor unit should capture 1 equiv of the added catalyst. The yield of the catalytic reactions should thus drop, representing an ^{int}ON state. After the addition of 1 equiv more of copper(I) ions, both 2-methylpyridine terminals of the biped ligand **2** should locate on the $Cu^I phenAr_2$ stations, exposing both ZnPor stations to capture the remaining catalyst from the solution. No further catalytic product formation is expected in the presence of $[Cu_2(\mathbf{1})(\mathbf{2})]^{2+}$, i.e., a catalytic OFF state.

For a proof of concept, we selected *N*-methylpyrrolidine (**10**) as the catalyst because it is able to catalyze the conjugate addition of thiophenol (**8**) to 2-cyclopentenone (**9**; Scheme 2). Moreover, **10** has a significant binding affinity toward the ZnPor unit (log K = 4.2)[35] of **1** so that its catalytic activity is

DOI: 10.1021/acs.inorgchem.7b02703
Inorg. Chem. XXXX, XXX, XXX−XXX

Scheme 2. Reaction Scheme for the Model Reaction

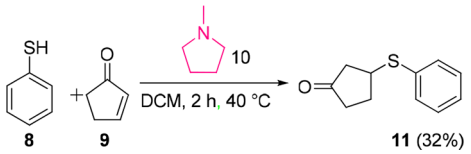

basically zero in a complex with the ZnPor unit. The switching of the overall catalytic machinery should then be visible from the amounts of product **11**.

Before in situ regulation of the conjugate addition reaction by the addition and removal of copper(I) ions in the full catalytic machinery (Scheme 3) was studied, several control experiments were undertaken. When the reaction of **8** and **9** (both 100 mol %) is run in the presence of 9 mol % organocatalyst **10** using standardized conditions [dichloromethane (DCM), 40 °C, 2 h], then product **11** is detected in (32 ± 2)% yield (Figure S22). In the presence of 4 mol % catalyst **10**, the yield is (16 ± 2)% (Figure S23). In contrast, no product **11** is formed in the presence of both zinc(II) tetraphenylporphyrin (**3**; 9 mol %) and **10** (9 mol %), confirming that formation of the strong complex [(**3**)(**10**)] inhibits the reaction between **8** and **9** (Figure S24).

After these model experiments, we studied the conjugated addition reaction in the presence of each individual state of the catalytic machinery. First, we examined the OFF state, i.e., CatState III (a six-component mixture). Here both free ZnPor stations of track **1** are expected to fully capture catalyst **10**, preventing catalysis. We mixed track **1**, biped ligand **2**, $[Cu(CH_3CN)_4]PF_6$, substrates **8** and **9**, and catalyst **10** in a 10:10:20:200:200:18 ratio in CD_2Cl_2 and heated the resulting solution at 40 °C for 2 h. No product formation was observed in the ^{1}H NMR, confirming that CatState III is indeed an OFF state for catalysis (Figure S29). Thereafter, we studied the formation of product **11** in the presence of CatState I as 100% ON state (for yield calculations, tetrachloroethane is used as an internal reference). After track **1**, biped ligand **2**, substrates **8** and **9**, and catalyst **10** were mixed in a 10:10:200:200:18 ratio in CD_2Cl_2, the mixture was heated for 2 h at 40 °C, furnishing (28 ± 2)% product **11** (Figure S27). Now, CatState II was evaluated for its catalytic activity. After track **1**, biped ligand **2**, and $[Cu(CH_3CN)_4]PF_6$were mixed in a 10:10:10 ratio in CD_2Cl_2 and substrates **8** and **9** and catalyst **10** were added in a 200:200:18 ratio, the mixture was heated at 40 °C for 2 h. Quantification by ^{1}H NMR analysis corroborated the product formation in (12 ± 2)% yield (Figure S28). Thus, CatState II indeed acts as an ^{int}ON state, demonstrating that the ZnPor unit in $[Cu(\mathbf{1})(\mathbf{2})]^+$ is able to capture a defined part of the catalyst, leaving the rest of the catalyst free in the solution.

Finally, the study of in situ product formation and inhibition during forward and backward walking of biped ligand **2** on track **1** was investigated (Figure 2). Hereunto, track **1** and biped ligand **2** (10:10) were mixed to form CatState I, and then substrates **8** and **9** and catalyst **10** (200:200:18) were added. The resulting mixture in CD_2Cl_2 was heated for 2 h in an NMR tube at 40 °C. ^{1}H NMR showed 27% product **11** (Figure S30a). Now 1 equiv of $[Cu(CH_3CN)_4]PF_6$ and the consumed amounts of substrates **8** and **9** were added. After heating, ^{1}H NMR showed 39% product **11** (Figure S30b), thus an increase by 12%. This finding indirectly confirms the formation of CatState II in solution (^{int}ON state) because the catalytic activity in solution has come to roughly half of that in CatState I. Finally, 1 equiv of $[Cu(CH_3CN)_4]PF_6$ and again the consumed amounts of **8** and **9** were added. After this mixture had been heated (2 h at 40 °C), ^{1}H NMR analysis still showed 39% product **11** (Figure S30c). Apparently, the present mixture represents an OFF state of catalysis, as we would expect for CatState III. To reverse the walking and to regenerate CatState II, 2 equiv of **7** was added as well as the consumed amounts of substrates **8** and **9**. Upon heating for 2 h at 40 °C, ^{1}H NMR analysis indicated an increase of the product yield by 12% (Figure S30d), in agreement with the formation of CatState II. The addition of 2 equiv more of **7** and used-up substrates gave rise to a 24% increase in product **11** (Figure S30e), in agreement with the regeneration of CatState I.

To challenge the reproducibility of the catalytic walker machinery, we now began the catalytic cycle with CatState III as the OFF state using the same stoichiometric ratios as before. We evaluated the product yields starting with CatState III, added the required amounts of **7** to probe CatStates II and I, and studied the backward cycle in the same mixture by the

Scheme 3. Cartoon Representation of the Stepwise (ON/^{int}ON/OFF) Regulation of a Conjugate Addition Reaction at the Different States (CatStates) by the Addition and Removal of Cu^+ Ions

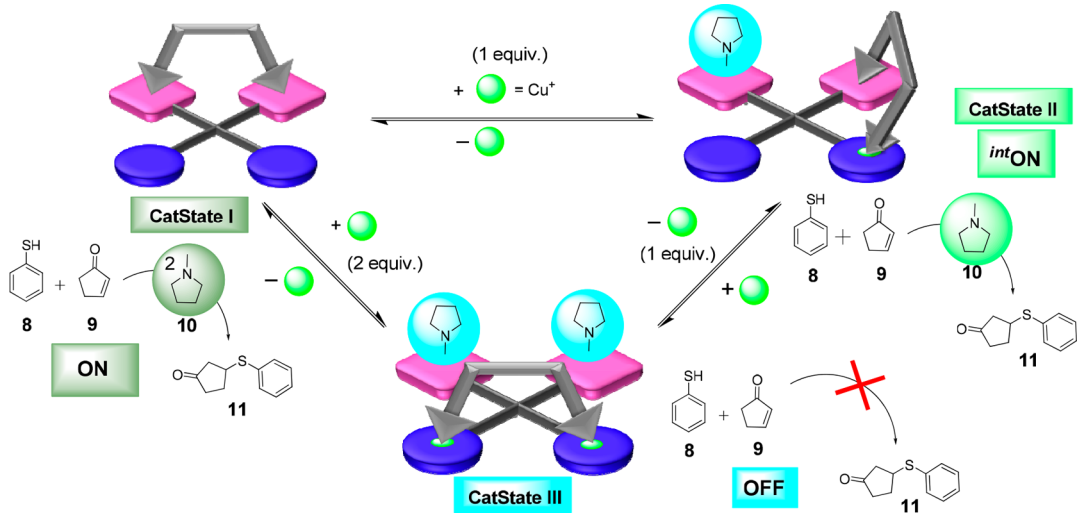

DOI: 10.1021/acs.inorgchem.7b02703
Inorg. Chem. XXXX, XXX, XXX−XXX

(a)

	% product 11 formation	
	Forward Cycle	Backward Cycle
CatState I (ON state)	27	24
CatState II (^{int}ON state)	12	12
CatState III (OFF state)	0	-

(b)

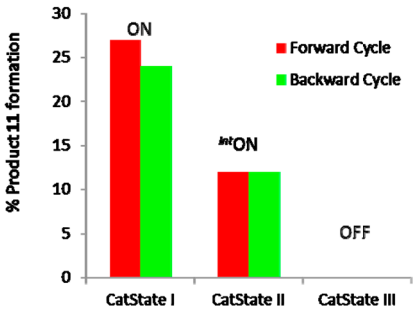

Figure 2. Product formation in each state in forward and backward cycles: (a) table; (b) bar graph representation.

addition of $[Cu(CH_3CN)_4]PF_6$, probing CatStates II and III. All CatStates were evaluated for their catalytic activity under standardized conditions (DCM, 40 °C, 2 h). The total yield of **11** in this sequence (0, 12%, 35%, 46%, and 48%) allows us to calculate the yields in the various CatStates: CatState III (0%) → CatState II (12%) → CatState I (23%) → CatState II (11%) → CatState III (2%) (Figure S31). An examination of the averaged yields for all in situ probed CatStates provides the following results: CatState I [(24.7 ± 2.1)%], CatState II [(11.75 ± 0.5)%], and CatState III [(0.3 ± 0.6)%]. As a result, CatState II furnishes 47.6% of the yield observed in CatState I, in good agreement with the different amounts of catalyst available under ideal walking behavior [CatState I (18 mol % catalyst), defined as 100%; CatState II (8 mol % out of 18 mol % of the catalyst should be available): 44.4%]. Thus, the yields obtained in the in situ forward and backward cycles reveal that the two-step walking of the biped ligand **2** on track **1** in the catalytic machinery is reversible, reproducible, and a means to successfully regulate the conjugate addition reaction in a systems-chemistry approach.[36]

■ CONCLUSIONS

In conclusion, a novel walker system based on metal−ligand binding and cleavage is designed as a special metallomacrocycle that changes its connectivity with each input.[37] Upon the addition/removal of copper(I) ions, the biped ligand **2** walks forward and backward on the tetrahedral track **1** from the ZnPor to $phenAr_2$ stations in two steps. The sequential addition and removal of copper ions allows access to all states of the system in a clean manner. The addition of **10** as the catalyst to the walker system generates a four-component catalytic machinery. After the addition of the required substrates, the different catalytic states were utilized to control a conjugate addition reaction in a stepwise manner by regulating the release and uptake of **10** as the catalyst. The present work is the first example, in which an artificial molecular walker system is able to regulate a catalytic reaction.[38] The regulation defines three different levels of catalytic activity from ON to ^{int}ON to OFF. Thus, the present catalytic ensemble that requires a mixture of seven components represents switchable and highly reliable advanced molecular machinery.

■ EXPERIMENTAL SECTION

General Information. All commercial reagents were used without further purification. Solvents were dried with the appropriate desiccants and distilled prior to use. ^{1}H and ^{13}C NMR were recorded on a Bruker Avance 400 (400 MHz) or on a Varian-S 600 (600 MHz) spectrometer using a deuterated solvent as the lock and a residual protiated solvent as the internal reference (CD_2Cl_2, δ_H = 5.32 ppm and δ_C = 53.8 ppm; $CDCl_3$, δ_H = 7.26 ppm and δ_C = 77.2 ppm). The following abbreviations were utilized to describe the peak patterns: s = singlet, d = doublet, t = triplet, dd = doublet of doublets, td = triplet of doublets, dt = doublet of triplets, br = broad, bs = broad singlet, bd = broad doublet, and m = multiplet. The numbering of the carbon atoms in the molecular formulas (vide infra) is used only for the assignments of the NMR signals and thus is not necessarily in accordance with IUPAC nomenclature. Electrospray ionization mass spectrometry (ESI-MS) spectra were recorded on a Thermo-Quest LCQ Deca spectrometer. Melting points were measured on a Büchi SMP-20 instrument. IR spectra were recorded using a Varian 1000 FT-IR instrument. UV−vis spectra were recorded on a Varian Cary 100 BioUV/Vis spectrometer. Elemental analysis was done on the EA 3000 CHNS analyzer.

Synthesis of State I. Track **1** (811 μg, 0.282 μmol) and biped ligand **2** (184 μg, 0.282 μmol) were loaded into an NMR tube and dissolved in CD_2Cl_2. The resultant mixture was subjected to characterization without any further purification. Yield: quantitative. ^{1}H NMR (400 MHz, CD_2Cl_2): δ 8.88 (d, ^3J = 4.6 Hz, 4H, β-H), 8.73 (d, ^3J = 4.6 Hz, 4H, β-H), 8.67 (s, 8H, β-H), 8.36 (d, ^3J = 8.4 Hz, 2H, [4/7]-H), 8.34 (d, ^3J = 8.2 Hz, 2H, [7/4]-H), 8.23 (d, ^3J = 8.2 Hz, 4H, [15/14]-H), 7.94 (d, ^3J = 8.2 Hz, 4H, [14/15]-H), 7.91 (s, 4H, 5- and 6-H), 7.68 (d, ^3J = 8.6 Hz, 4H, [13/10]-H), 7.62 (d, ^3J = 8.7 Hz, 4H, [10/13]-H), 7.57 (d, ^3J = 8.4 Hz, 2H, [3/8]-H), 7.56 (d, ^3J = 8.2 Hz, 2H, [8/3]-H), 7.54 (t, ^3J = 1.6 Hz, 2H, g-H), 7.47 (dt, ^3J = 7.6 Hz, ^4J = 1.6 Hz, 2H, [d/f]-H), 7.43 (d, ^3J = 8.7 Hz, 4H, [11/12]-H), 7.40 (d, ^3J = 8.6 Hz, 4H, [12/11]-H), 7.37 (dt, ^3J = 7.6 Hz, ^4J = 1.6 Hz, 2H, [f/d]-H), 7.31 (t, ^3J = 7.6 Hz, 2H, e-H), 7.28 (s, 12H, 16- and 17-H), 6.98 (s, 2H, h-H), 6.97 (s, 4H, 9-H), 6.61 (s, 2H, c-H), 6.52 (d, ^3J = 5.6 Hz, 2H, b-H), 5.98 (br, 2H, a-H), 3.99 (t, ^3J = 6.4 Hz, 4 H, i-H), 2.61 (s, 18H, f′- and h′-H), 2.57 (s, 12H, [b′/a′]-H), 2.34 (s, 6H, d′-H), 2.05 (s, 12H, c′-H), 1.96 (s, 12H, [a′/b′]-H), 1.82 (s, 12H, g′-H), 1.81 (s, 24H, e′-H), 1.82−1.75 (m, 4 H, j-H), 1.58−1.48 (m, 4 H, k-H), 0.96 (m, 12 H, Me- and l-H). IR (KBr): ν 3435, 2950, 2920, 2850, 2211, 1599, 1503, 1478, 1379, 1337, 1279, 1203, 1062, 995, 852, 826, 797, 725 cm^{-1}. UV−vis (CH_2Cl_2): λ_{max} = 560 nm (Q band; ε = 1.43 × 10^4 M^{-1} cm^{-1}). Anal. Calcd for $C_{247}H_{204}N_{14}O_2Zn_2{\cdot}2CH_2Cl_2$: C, 80.81; H, 5.66; N, 5.30. Found: C, 81.15; H, 5.53; N, 5.19.

Synthesis of State II. Track **1** (1.71 mg, 0.594 μmol), biped ligand **2** (388 μg, 0.594 μmol), and $[Cu(CH_3CN)_4]PF_6$ (221 μg, 0.594 μmol) were loaded into an NMR tube and dissolved in CD_2Cl_2. The resultant mixture was subjected to analytical characterization without any further purification. Yield: quantitative. ^{1}H NMR (400 MHz, CD_2Cl_2) of two diastereomers in a ratio of 1:1 (diastereotopic characteristic protons marked as asterisks and subscript C and UC in proton assignments are used for complexed and uncomplexed phenanthroline, respectively): δ = 8.86 (d, ^3J = 4.8 Hz, 1H, β-H), 8.83−8.81 (m, 3H, β-H), 8.74−8.62 (m, 14H, 4_C-, 7_C- and β-H), 8.38−8.32 (m, 2H, 4_{UC}- and 7_{UC}-H), 8.23−8.15 (m, 6H, 5_C-, 6_C-, and [14/15]-H), 7.96−7.88 (m, 8H, 8_C-, 3_C-, 5_{UC}-, 6_{UC}-, and -[15/14]-H), 7.69−7.50 (m, 12H, g-, 13-, 14-, 3_{UC}-, 8_{UC}-, d-, and f-H), 7.44−7.39 (m, 4H, 11- and 12-H), 7.34−7.18 (m, 8H, e-, c-, and mes-H), 7.05 (s, 2H, h-H), 6.96 (s, 1H, 9_{UC}*-H), 6.95 (s, 1H, 9_{UC}-H), 6.82 (bs, 2H, b-H), 6.75 (s, 1H, 9_C*-H), 6.72 (bs, 3H, a- and 9_C-H), 4.01 (t, ^3J = 6.0 Hz, 4H, i-H), 2.60 (s, 18H, f′- and h′-H), 2.56 (s, 3H, $[b'/a']_{UC}$*-H), 2.54 (s, 3H, $[b'/a']_{UC}$-

DOI: 10.1021/acs.inorgchem.7b02703
Inorg. Chem. XXXX, XXX, XXX−XXX

H), 2.38 (s, 3H, [b′/a′]$_C$*-H), 2.36 (s, 3H, [b′/a′]$_C$-H), 2.34 (s, 1.5H, d′$_{UC}$*-H), 2.32 (s, 1.5H, d′$_{UC}$-H), 2.15 (s, 3H, d′$_C$-H), 2.05 (s, 3H, c′$_{UC}$*-H), 2.04 (s, 3H, c′$_{UC}$-H), 2.02 (s, 6H, c′$_C$-H), 1.96 (s, 3H, [a′/b′]$_{UC}$*-H), 1.94 (s, 3H, [a′/b′]$_{UC}$-H), 1.92 (bs, 6H, [a′/b′]$_C$-H), 1.82−1.77 (m, 40H, j-, g′-, and e′-H), 1.57−1.47 (m, 10H, k- and Me-H), 0.94 (t, ^3J = 7.2 Hz, 6H, l-H). IR (KBr): ν 3436, 2922, 2858, 2219, 1641, 1610, 1511, 1463, 1376, 1333, 1272, 1220, 1202, 1083, 1060, 997, 979, 852, 829, 798 cm^{-1}. UV−vis (CH_2Cl_2): λ_{max} = 554 nm (Q band; ε = 1.46 × 10^4 M^{-1} cm^{-1}). Anal. Calcd for $C_{247}H_{204}CuF_6N_{14}O_2PZn_2{\cdot}2.5CH_2Cl_2$: C, 75.83; H, 5.33; N, 4.96. Found: C, 75.59; H, 4.94; N, 4.69.

Synthesis of State III. Track **1** (811 μg, 0.282 μmol), biped ligand **2** (184 μg, 0.282 μmol), and [Cu(CH$_3$CN)$_4$]PF$_6$ (210 μg, 0.564 μmol) were loaded in an NMR tube and dissolved in CD_2Cl_2. The resultant mixture was subjected to characterization without any further purification. Yield: quantitative. ^{1}H NMR (400 MHz, CD_2Cl_2): δ 8.89 (d, ^3J = 4.6 Hz, 4H, β-H), 8.76 (d, ^3J = 4.6 Hz, 4H, β-H), 8.75−8.69 (m, 12H, β-, 4-, and 7-H), 8.23 (d, ^3J = 7.6 Hz, 2H, [15/14]-H), 8.21 (s, 4H, 5- and 6-H), 7.95 (d, ^3J = 8.4 Hz, 2H, [3/8]-H), 7.94 (d, ^3J = 8.4 Hz, 2H, [8/3]-H), 7.90 (d, ^3J = 7.6 Hz, 4H, [14/15]-H), 7.81 (bs, 2H, g-H), 7.62−7.48 (m, 14H, a-, d-, f-, 10-, and 13-H), 7.43−7.30 (m, 10H, 11-, 12-, and e-H), 7.29 (s, 6H, 16- and 17-H), 7.17 (bs, 2H, c-H), 7.12 (s, 2H, h-H), 7.06 (bd, 2H, b-H), 6.71 (s, 4H, 9-H), 4.00 (t, ^3J = 6.0 Hz, 4H, i-H), 2.61 (s, 18H, f′- and h′-H), 2.41 (s, 12H, [b′/a′]-H), 2.15 (s, 6H, d′-H), 2.02 (s, 12H, c′-H), 1.93 (s, 12H, [a′/b′]-H), 1.92 (s, 6H, Me-H), 1.84 (s, 12H, g′-H), 1.83 (s, 24H, e′-H), 1.76−1.72 (m, 4 H, j-H), 1.49−1.46 (m, 4 H, k-H), 0.88 (t, 6 H, l-H). IR (KBr): ν 3435, 2920, 2213, 1642, 1612, 1512, 1463, 1376, 1336, 1275, 1204, 1085, 998, 979, 892, 853, 826, 799, 774, 756, 725 cm^{-1}. ESI-MS: m/z (%) 1829.1 (100; [M − 2PF$_6$]$^{2+}$). UV−vis (CH_2Cl_2): λ_{max} = 550 nm (Q band; ε = 1.36 × 10^4 M^{-1} cm^{-1}). Anal. Calcd for $C_{247}H_{204}Cu_2F_{12}N_{14}O_2P_2Zn_2{\cdot}3CH_2Cl_2$: C, 71.44; H, 5.04; N, 4.67. Found: C, 71.24; H, 4.71; N, 4.58.

In Situ Cycle 1 Starting with CatState I. The forward catalytic reaction was started with CatState I prepared directly in the NMR tube. Track **1** (830 μg, 0.288 μmol) and biped ligand **2** (188 μg, 0.288 μmol) were dissolved in 500 μL of CD_2Cl_2. To generate CatState I, compounds **8** (635 μg, 5.76 μmol), **9** (470 μg, 5.76 μmol), and **10** (44.1 μg, 0.518 μmol) were added and the resultant mixture was heated at 40 °C for 2 h. The reaction mixture was then cooled to 0 °C (to stop the reaction) and immediately subjected to ^{1}H NMR analysis. The formation of product **11** (27%) was observed (100% ON; Figure S30a). Thereafter, 1 equiv of [Cu(CH$_3$CN)$_4$]PF$_6$ (107 μg, 0.288 μmol) was added along with the consumed amounts of substrates **8** and **9** (CatState II). The mixture was heated for 2 h at 40 °C. The total yield of product **11** improved to 39%, indicating an increase by 12% (^{int}ON; Figure S30b). Again 1 equiv more of [Cu(CH$_3$CN)$_4$]PF$_6$ (107 μg, 0.288 μmol) and the consumed amounts of substrates **8** and **9** were added (CatState III). After heating for 2 h at 40 °C, no further increase in the yield of product **11** (total of 39%) was observed in the NMR (Figure S30c). Now backward walking was initiated by the addition of **7** (278 μg, 0.576 μmol) and the used-up **8** and **9**. The thus-generated CatState II led to a total yield of 51% of **11**, thus a 12% increase (Figure S30d). To regenerate CatState I, 2 equiv more of **7** (278 μg, 0.576 μmol) and the consumed amounts of substrates **8** and **9** were added. The mixture was subjected to heating at 40 °C for 2 h. The total yield of 75% product **11** was observed in ^{1}H NMR (Figure S30e).

In Situ Cycle 2 Starting with CatState III. To prepare CatState III directly in the NMR tube, track **1** (800 μg, 0.278 μmol), biped ligand **2** (181 μg, 0.278 μmol), and [Cu(CH$_3$CN)$_4$]PF$_6$ (207 μg, 0.556 μmol) were dissolved in 500 μL of CD_2Cl_2. Compounds **8** (613 μg, 5.56 μmol), **9**(461 μg, 5.56 μmol), and **10** (42.6 μg, 0.500 μmol) were then added, and the mixture was heated at 40 °C for 2 h. The reaction mixture was immediately subjected to ^{1}H NMR measurement after cooling to 0 °C to stop the reaction. No formation of product **11** was observed (Figure S31a). Thereafter, 2 equiv of **7** (268 μg, 0.556 μmol) was added and the sample heated again for 2 h at 40 °C. Now 12% yield of product **11** was observed (^{int}ON; Figure S31b). Again 2 equiv more of **7** (268 μg, 0.556 μmol) and the consumed amounts of substrates **8** and **9** were added. After heating for 2 h at 40 °C, a further increase in the yield of product **11** (total of 35%) was observed in the NMR (Figure S31c). To start the reverse cycle, 1 equiv of [Cu(CH$_3$CN)$_4$]PF$_6$ (103 μg, 0.278 μmol) and the used-up **8** and **9** were added to regenerate CatState II. After heating, a further increase in the yield of product **11** (total of 46%) was observed in the NMR (Figure S31d). Now, to regenerate CatState III (OFF state), 1 equiv more of [Cu(CH$_3$CN)$_4$]PF$_6$ (103 μg, 0.278 μmol) and the consumed amounts of substrates **8** and **9** were added. After heating for 2 h at 40 °C, a minute (2%) increment in the product yield of **11** was observed (Figure S31e).

■ ASSOCIATED CONTENT

Supporting Information

The Supporting Information is available free of charge on the ACS Publications website at DOI: 10.1021/acs.inorgchem.7b02703.

Synthesis and characterization of **1** and **2**, spectroscopic data for all new complexes and ligands, and all catalytic experiments and controls (PDF)

■ AUTHOR INFORMATION

Corresponding Author

*E-mail: schmittel@chemie.uni-siegen.de.

ORCID

Michael Schmittel: 0000-0001-8622-2883

Notes

The authors declare no competing financial interest.

■ ACKNOWLEDGMENTS

We are highly indebted to the DFG (Schm 647/19-2 and 20-1) and the University of Siegen for their continued support of this research.

■ DEDICATION

This work is dedicated to Prof. Dr. W. H. E. Schwarz on the occasion of his 80th birthday.

■ REFERENCES

(1) Abendroth, J. M.; Bushuyev, O. S.; Weiss, P. S.; Barrett, C. J. Controlling Motion at the Nanoscale: Rise of the Molecular Machines. *ACS Nano* **2015**, *9*, 7746−7768.

(2) Hirokawa, N. Kinesin and Dynein superfamily proteins and the mechanism of organelle transport. *Science* **1998**, *279*, 519−526.

(3) Vale, R. D.; Milligan, R. A. The way things move: looking under the hood of molecular motor proteins. *Science* **2000**, *288*, 88−95.

(4) Vale, R. D. The molecular motor toolbox for intercellular transport. *Cell* **2003**, *112*, 467−480.

(5) Schliwa, M.; Woehlke, G. Molecular motors. *Nature* **2003**, *422*, 759−765.

(6) Amos, L. A. Molecular motors: Not quite like clockwork. *Cell. Mol. Life Sci.* **2008**, *65*, 509−515.

(7) Otto, S. Molecular machines: Tiny steps. *Nat. Chem.* **2010**, *2*, 75−76.

(8) Barrell, M. J.; Campaňa, A. G.; von Delius, M.; Geertsema, E. M.; Leigh, D. A. Light-driven transport of a molecular walker in either direction along a molecular track. *Angew. Chem., Int. Ed.* **2011**, *50*, 285−290.

(9) von Delius, M.; Leigh, D. A. Walking molecules. *Chem. Soc. Rev.* **2011**, *40*, 3656−3676.

(10) Qu, D.-H.; Tian, H. Synthetic small-molecule walkers at work. *Chem. Sci.* **2013**, *4*, 3031−3035.

(11) Leigh, D. A.; Lewandowska, U.; Lewandowski, B.; Wilson, M. R. Synthetic molecular walkers. *Top. Curr. Chem.* **2014**, *354*, 111−138.

DOI: 10.1021/acs.inorgchem.7b02703
Inorg. Chem. XXXX, XXX, XXX−XXX

(12) Kovaříček, P.; Lehn, J.-M. Directional Dynamic Covalent Motion of a Carbonyl Walker on a Polyamine Track. *Chem. - Eur. J.* **2015**, *21*, 9380−9384.
(13) Pulcu, G. S.; Mikhailova, E.; Choi, L.-S.; Bayley, H. Continuous observation of the stochastic motion of an individual small-molecule walker. *Nat. Nanotechnol.* **2015**, *10*, 76−83.
(14) Martin, C. J.; Lee, A. T. L.; Adams, R. W.; Leigh, D. A. Enzyme-Mediated Directional Transport of a Small-Molecule Walker With Chemically Identical Feet. *J. Am. Chem. Soc.* **2017**, *139*, 11998−12002.
(15) Schmittel, M. From self-sorted coordination libraries to networking nanoswitches for catalysis. *Chem. Commun.* **2015**, *51*, 14956−14968.
(16) Beves, J. E.; Blanco, V.; Blight, B. A.; Carrillo, R.; D'Souza, D. M.; Howgego, D.; Leigh, D. A.; Slawin, A. M. Z.; Symes, M. D. Toward metal complexes that can directionally walk along tracks: Controlled stepping of a molecular biped with a palladium(II) foot. *J. Am. Chem. Soc.* **2014**, *136*, 2094−2100.
(17) Campaña, A. G.; Carlone, A.; Chen, K.; Dryden, D. T. F.; Leigh, D. A.; Lewandowska, U.; Mullen, K. M. A small molecule that walks non-directionally along a track without external intervention. *Angew. Chem., Int. Ed.* **2012**, *51*, 5480−5483.
(18) Lewandowski, B.; De Bo, G.; Ward, J. W.; Papmeyer, M.; Kuschel, S.; Aldegunde, M. J.; Gramlich, P. M. E.; Heckmann, D.; Goldup, S. M.; D'Souza, D. M.; Fernandes, A. E.; Leigh, D. A. Sequence-specific peptide synthesis by an artificial small-molecule machine. *Science* **2013**, *339*, 189−193.
(19) Schmittel, M.; De, S.; Pramanik, S. Reversible ON/OFF nanoswitch for organocatalysis: mimicking the locking and unlocking operation of CaMKII. *Angew. Chem., Int. Ed.* **2012**, *51*, 3832−3836.
(20) De, S.; Pramanik, S.; Schmittel, M. A toggle nanoswitch alternately controlling two catalytic reactions. *Angew. Chem., Int. Ed.* **2014**, *53*, 14255−14259.
(21) Gaikwad, S.; Goswami, A.; De, S.; Schmittel, M. A Metal-loregulated Four-State Nanoswitch Controls Two-Step Sequential Catalysis in an Eleven-Component System. *Angew. Chem., Int. Ed.* **2016**, *55*, 10512−10517.
(22) Mahata, K.; Schmittel, M. From 2-fold completive to integrative self-sorting: a five-component supramolecular trapezoid. *J. Am. Chem. Soc.* **2009**, *131*, 16544−16554.
(23) Wiley, C. A.; Holloway, L. R.; Miller, T. F.; Lyon, Y.; Julian, R. R.; Hooley, R. J. Electronic Effects on Narcissistic Self-Sorting in Multicomponent Self-Assembly of Fe-Iminopyridine meso-Helicates. *Inorg. Chem.* **2016**, *55*, 9805−9815.
(24) Biswas, P. K.; Saha, S.; Nanaji, Y.; Rana, A.; Schmittel, M. Influence of Rotator Design on the Speed of Self-Assembled Four-Component Nanorotors: Coordinative Versus Dispersive Interactions. *Inorg. Chem.* **2017**, *56*, 6662−6670.
(25) Saha, M. L.; Schmittel, M. Metal-Ligand Exchange in a Cyclic Array: The Stepwise Advancement of Supramolecular Complexity. *Inorg. Chem.* **2016**, *55*, 12366−12375.
(26) Goswami, A.; Paul, I.; Schmittel, M. Three-component nanorotors generated from fusion of complexes and post-fusion metal-metal exchange. *Chem. Commun.* **2017**, *53*, 5186−5189.
(27) Samanta, D.; Paul, I.; Schmittel, M. Supramolecular five-component nano-oscillator. *Chem. Commun.* **2017**, *53*, 9709−9712.
(28) Favereau, L.; Cnossen, A.; Kelber, J. B.; Gong, J. Q.; Oetterli, R. M.; Cremers, J.; Herz, L. M.; Anderson, H. L. Six-Coordinate Zinc Porphyrins for Template-Directed Synthesis of Spiro-Fused Nanorings. *J. Am. Chem. Soc.* **2015**, *137*, 14256−14259.
(29) Liu, S.; Kondratuk, D. V.; Rousseaux, S. A. L.; Gil-Ramírez, G.; O'Sullivan, M. C.; Cremers, J.; Claridge, T. D. W.; Anderson, H. L. Caterpillar Track Complexes in Template-Directed Synthesis and Correlated Molecular Motion. *Angew. Chem., Int. Ed.* **2015**, *54*, 5355.
(30) Saha, B.; Ikbal, S. A.; Petrovic, A. G.; Berova, N.; Rath, S. P. Complexation of Chiral Zinc-Porphyrin Tweezer with Achiral Diamines: Induction and Two-Step Inversion of Interporphyrin Helicity Monitored by ECD. *Inorg. Chem.* **2017**, *56*, 3849−3860.
(31) Neogi, S.; Schnakenburg, G.; Lorenz, Y.; Engeser, M.; Schmittel, M. Implications of stoichiometry-controlled structural changeover between heteroleptic trigonal $[Cu(phenAr_2)(py)]^+$ and tetragonal $[Cu(phenAr_2)(py)_2]^+$ motifs for solution and solid-state supramolecular self-assembly. *Inorg. Chem.* **2012**, *51*, 10832−10841.
(32) Kirksey, C. H.; Hambright, P.; Storm, C. B. Stability constants and proton magnetic resonance studies of zinc $\alpha,\beta,\gamma,\delta$-tetraphenylporphin and substituted pyridines. *Inorg. Chem.* **1969**, *8*, 2141−2144.
(33) The 4-nm shift in state II, i.e., midway between states I and III, indicates that one foot of the biped oscillates rapidly between the two ZnPor stations, as described in other systems.[27]
(34) Saha, M. L.; Mittal, N.; Bats, J. W.; Schmittel, M. A six-component metallosupramolecular pentagon via self-sorting. *Chem. Commun.* **2014**, *50*, 12189−12192.
(35) Mittal, N.; Pramanik, S.; Paul, I.; De, S.; Schmittel, M. Networking Nanoswitches for ON/OFF Control of Catalysis. *J. Am. Chem. Soc.* **2017**, *139*, 4270−4273.
(36) Ashkenasy, G.; Hermans, T. M.; Otto, S.; Taylor, A. F. Systems chemistry. *Chem. Soc. Rev.* **2017**, *46*, 2543−2554.
(37) Holloway, L. R.; McGarraugh, H. H.; Young, M. C.; Sontising, W.; Beran, G. J. O.; Hooley, R. J. Structural switching in self-assembled metal−ligand helicate complexes via ligand-centered reactions. *Chem. Sci.* **2016**, *7*, 4423−4427.
(38) Erbas-Cakmak, S.; Leigh, D. A.; McTernan, C. T.; Nussbaumer, A. L. Artificial Molecular Machines. *Chem. Rev.* **2015**, *115*, 10081−10206.

DOI: 10.1021/acs.inorgchem.7b02703
Inorg. Chem. XXXX, XXX, XXX−XXX